Time-resolved x-ray magnetic circular dichroism study of ultrafast demagnetization in a CoPd ferromagnetic film excited by circularly polarized laser pulse

Víctor López-Flores,[1,*] Jacek Arabski,[1] Christian Stamm,[2] Valérie Halté,[1] Niko Pontius,[2] Eric Beaurepaire,[1] and Christine Boeglin[1,†]

[1]*Institut de Physique et Chimie des Matériaux de Strasbourg, UMR7504, CNRS–Université de Strasbourg, 67034 Strasbourg, France*

[2]*Institut für Methoden und Instrumentierung der Forschung mit Synchrotronstrahlung, Helmholtz-Zentrum Berlin für Materialien und Energie GmbH, Albert-Einstein-Straße 15, 12489 Berlin, Germany*

(Received 13 January 2012; published 23 July 2012)

The magnetization dynamics of CoPd films excited by circularly polarized ultrashort laser pulses is studied by time-resolved x-ray magnetic circular dichroism. In those films the ultrafast dynamics measured at the Co-L_3 edge is strongly sensitive to the orbital magnetic moment L_z. The amount of angular momentum transferred by the circularly polarized ultrashort laser pulses to the ferromagnetic films is evaluated to $\pm 0.1\,\hbar$/atom, which is above the detection limit of the experiment. Despite this, no polarization-dependent difference on the magnetization dynamics could be evidenced. These results are explained by ultrafast electronic relaxation mechanisms of the transferred angular momentum, faster than $\sim$100 fs. This experiment sets the methodology as well as an upper time limit for determination of angular momentum relaxation processes.

DOI: 10.1103/PhysRevB.86.014424 PACS number(s): 75.78.Jp, 78.20.Ls, 78.47.J−

I. INTRODUCTION

Since its discovery in 1996,[1] a large number of studies have been devoted to understand the ultrafast magnetization dynamics induced by femtosecond laser pulses, due to the importance of its potential applications such as ultrafast magnetic recording media.[2–4] Many of these works study the magnetic effects induced by the energy transferred to electronic, spin, and lattice systems in the 100 fs–10 ps time range. In addition, nonthermal magnetic effects, such as, for instance, the inverse Faraday effect[3] or angular momentum transfer,[5] may occur in the femto- and picosecond time scale. In the last decade these ultrafast magnetization dynamics led to intensive work and controversies where the origin and mechanisms were debated.[2,6–10] The initial model describing the transfer of energy is the three-temperature model.[1] Nevertheless, a microscopic description of the mechanisms responsible for the transfer and conservation of the total angular momentum is still motivating intensive experimental and theoretical studies.[10] Behind those fundamental questions we also would like to know how fast magnetization relaxation can ultimately be.

Angular momentum can be directly transferred via dipolar selection rules by absorption of femtosecond circularly polarized pump pulses,[11] which can be used to study the mechanisms of ultrafast magnetization dynamics. The first attempts to experimentally detect the influence of the pump polarization have shown that, in addition to the laser-induced ultrafast demagnetization, there is a nonmagnetic polarization-dependent response. This latter effect is attributed to a coherent transfer of the angular momentum $(+\hbar, -\hbar)$ from the circularly polarized light $(\sigma+, \sigma-)$ to the electron orbital momentum[12,13] or by coherent magnetic response of the ferromagnet to the pump pulse.[2] All these experiments rely on time-resolved magneto-optical Kerr-effect (TR-MOKE) measurements. This technique accounts for changes in the rotation and ellipticity of a laser pulse probe, which are afterwards related to the actual average magnetization of the sample. However, this relationship has sometimes been debated for not being accurate for time delays below $\sim$1 ps,[7,14] as this method can detect nonmagnetic effects as well.

The objective of this work is to introduce a different experimental approach in the study of the transfer of angular momentum from the circularly polarized femtosecond laser pulse to the electrons in the ultrafast demagnetization process of a ferromagnetic material. Specifically, we will use a probe technique based on soft x-ray absorption that overcomes the problems of the above-mentioned laser probes. Time-resolved x-ray magnetic circular dichroism (TR-XMCD) has proved to be a useful technique to study the ultrafast demagnetization dynamics.[15–17] It has several advantages over TR-MOKE measurements, such as the capability of probing the magnetization per atom of a sample, with element selectivity. But the most relevant feature is that it can discriminate between the orbital and spin contribution to the magnetization by using the sum rules.[18] This means that its results are a direct measurement of the electronic magnetic moments with chemical and orbital selectivity. TR-XMCD using the slicing facility[19,20] provides a time resolution of about 100 fs, so it is an ideal tool to search for light-induced effects in the ultrafast region below 1 ps. In our previous work, we used this technique to show independently the ultrafast dynamics of the spin and orbital magnetic moments in a ferromagnetic CoPd alloy thin film with an unprecedented time resolution.[17] In the present study, we will follow the possible differences in the dynamics due to the different pump laser helicities $(\sigma+, \sigma-)$ in the same sample and compare with the experimental results coming from TR-MOKE measurements published elsewhere.[12,13]

II. EXPERIMENT

For this experiment, we chose a sample with a large out-of-plane magnetic anisotropy, related to a high orbital magnetic moment along the normal of the surface. This will enhance the detection of the possible effects on the orbital magnetic moment, allowing measurements in the more convenient perpendicular geometry.

The sample was a 15-nm-thick layer of a $Co_{0.5}Pd_{0.5}$ alloy, grown on a Si_3N_4 (200 nm) membrane on a Si frame, which allowed the transmission XMCD experiment. This thickness of the layer was chosen to ensure that the laser pumped the whole magnetic layer. The sample was prepared by electron beam coevaporation of Co and Pd from highly pure target metals. Base pressure was 1×10^{-9} mbar, and the deposition was made at room temperature. Thickness of the sample was monitored by calibrated quartz-crystal microbalances. A 20 nm Cu buffer layer was used to provide a good conductive layer so as to efficiently transfer the heat load coming from the pump laser. A 3 nm Cr capping layer was used to prevent oxidation of the magnetic layer from the atmosphere during sample transport. X-ray absorption spectroscopy (XAS) measurements ensured that there was no Co oxidation before and after the time-resolved experiment.

The time-resolved pump-probe XMCD experiment[15,16] was performed at the UE56/1-ZPM Femtoslicing beamline at the synchrotron BESSY II of the Helmholtz Zentrum Berlin. This beamline uses a Bragg-Fresnel reflection zone plate as a single optical element that disperses the energy and focuses the beam in order to achieve a very efficient x-ray transmission.[21] Soft x-ray pulses of about 100 fs duration with variable helicity and tunable photon energy are produced by means of femtosecond slicing: a femtosecond laser pulse that copropagates with an electron bunch in the storage ring leads to an energy modulation of the electrons, which subsequently radiate femtosecond x-ray pulses as they pass through the undulator.[19,22] This slicing laser comes from the splitting of the pump laser used to demagnetize the samples, so the x-ray pulses are intrinsically synchronized with the pump pulse. This pump laser is an amplified Ti:sapphire laser system operating at 790 nm wavelength and 60 fs pulse duration. The laser has a repetition rate of 3 kHz for the femtosecond x-ray generation, and 1.5 kHz for pumping the sample at the experiment. On the sample we have a measured fluence of 12 mJ/cm^2, with a spot size of 1.0×0.8 mm^2, larger than the x-ray spot of 0.3×0.1 mm^2 in order to probe homogeneously the pumped region. Both beams have nearly perpendicular incidence on the sample, with an angle of 1° in between them. The pump laser was circularly polarized using an adjustable polarizer that allows a fast change between left- and right-handed helicity ($\sigma+$ and $\sigma-$). This polarization was measured to be above 98% after the last mirror just before the sample.

XMCD data were taken at the Co-L_3 edge energy (778 eV) with left-handed circularly polarized x-ray pulses by switching the direction of the saturated magnetization of the sample at each pump-probe delay time, which ensured a reliable XMCD signal calculation while reducing the acquisition time. The latter is a critical issue in the experiment, as a good signal-to-noise ratio for one delay scan is obtained only after several days of acquisition. The magnetic saturation of the sample was obtained by applying a magnetic field of 0.4 T, oriented perpendicular to the surface.

The four experimental configurations used in transmission measurements are given by the laser light polarization vector and the x-ray polarization direction. They are illustrated in Fig. 1. The laser and x-ray beams are collinear and nearly parallel to the normal to the sample surface. Using linearly polarized pump laser light one would have performed the measurement subtracting two XAS signals from configurations (a) and (c) to obtain the XMCD. Using circular light this would lead to $XMCD_{\sigma+}$ combining the XAS from configurations (a) and (c) and $XMCD_{\sigma-}$ combining the XAS from (b) and (d). However, due to the broken symmetry using circular polarized laser light as a pump we have to combine situations (a) and (d), to calculate the "parallel" $XMCD_{par}$ and configurations (b) and (c) to calculate the "antiparallel" $XMCD_{ant}$ signal (referring to the respective direction of the magnetization and laser helicity). Using these combinations we are sensitive to an additive or subtractive contribution from the circular pump to the total orbital moment.

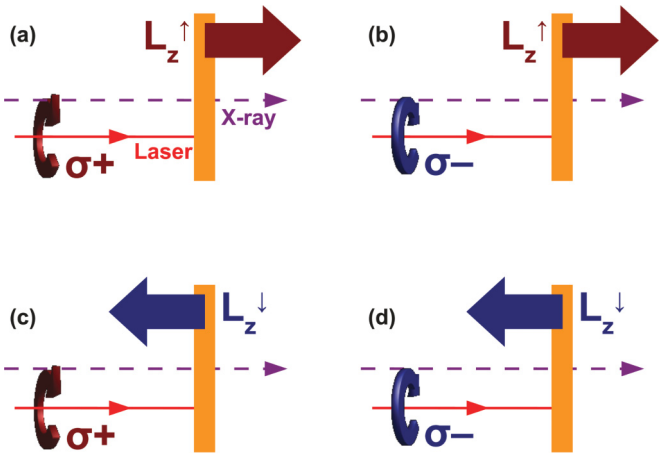

FIG. 1. (Color online) Experimental configuration of laser pump and x-ray probe beam with respect to the magnetization direction of the CoPd film. Four combinations of magnetization and laser angular moment are possible. (a) Positive magnetization and right-handed laser helicity; (b) positive magnetization and left-handed laser helicity; (c) negative magnetization and right-handed laser helicity; and (d) negative magnetization and left-handed laser helicity.

III. RESULTS

Figure 2(a) shows the ultrafast dynamic response of the experimental XMCD signal obtained at the Co-L_3 edge and recorded for opposite laser helicities ($\sigma+$ and $\sigma-$). The data represents the XMCD signal obtained from the difference of two transmission XAS signals obtained for two opposite magnetization directions, measured using a single pump helicity [Figs. 1(a) and 1(c), or 1(b) and 1(d)]. Both $XMCD_{\sigma+}$ and $XMCD_{\sigma-}$ dynamics show an ultrafast quenching (of ~55% of the original signal in this case) induced by the laser pump after $t = 0$. Using the same laser fluence of 12 mJ/cm^2 used in our previous work[17] we find the same demagnetization amplitude and characteristic times of the XMCD signal at the Co-L_3 edge in this experiment. This characteristic time was defined in our previous experiment by a linear combination of $L_z(t)$ and $S_z(t)$ for which it is possible to use the two-temperature model and extract 220 and 280 fs as thermalization times for orbital and spin moments, respectively. Recovery of the initial magnetization and XMCD at Co-L_3 is achieved for time scales corresponding to electron-phonon relaxation and heat diffusion processes in the pico- and nanosecond time ranges.[17] The inset of Fig. 2(a) shows the x-ray transmission signals (XAS) at the Co-L_3 edge used for the XMCD calculation.

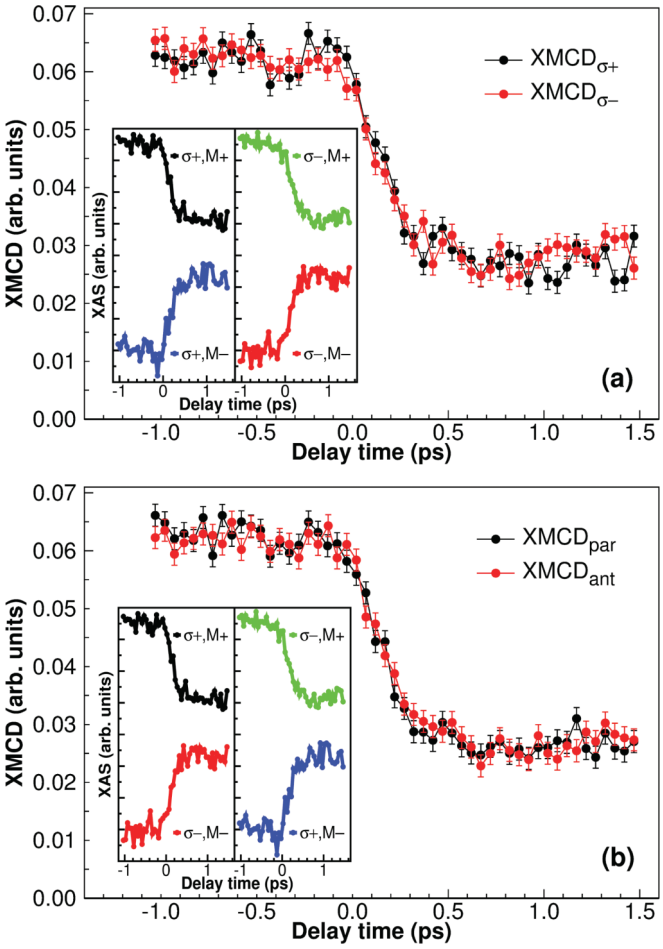

FIG. 2. (Color online) Experimental time-resolved measurements of Co-L_3 XMCD, obtained from the transmission signal as explained in the text. (a) Dynamic XMCD initiated by right- ($\sigma+$, black points) and left- ($\sigma-$, red points) handed pump laser helicity. (b) Two XMCD ultrafast dynamics where we subtract the positive sample magnetization, right-handed laser helicity ($\sigma+$) XAS signal from the negative sample magnetization, left-handed laser helicity ($\sigma-$) XAS signal defining the black data points called XMCD parallel (XMCD$_{par}$). The red data points are obtained by subtracting the positive sample magnetization, left-handed laser helicity XAS signal from the negative sample magnetization, right-handed laser helicity XAS, defining the points called XMCD antiparallel (XMCD$_{ant}$). The errors bars of the experimental data points are the standard deviation of the data points. Insets show the XAS signals used to calculate the respective XMCD values.

In order to observe specific transfer of angular momentum toward $L_z(t)$, the ultrafast dynamics using XMCD at Co-L_3 has to be measured by a specific combination between the momentum of the light and the orbital moment orientation. To do this, it is mandatory to extract from the previous data in Fig. 2(a) the two XMCD combinations where the pump helicity is either parallel or antiparallel to the orbital moment orientation, defined by the applied external magnetic field. This corresponds to Figs. 1(a) and 1(d) for the parallel signal, and Figs. 1(b) and 1(c) for the antiparallel signal.

In Fig. 2(b), we show the two XMCD ultrafast dynamics, where we subtract the positive sample magnetization, right-handed laser helicity ($\sigma+$) XAS signal [Fig. 1(d) configuration] from the negative sample magnetization, left-handed laser helicity ($\sigma-$) XAS signal [Fig. 1(a) configuration], defining the black data points called XMCD parallel (XMCD$_{par}$). The red data points are obtained by subtracting the positive sample magnetization, left-handed laser helicity XAS signal [Fig. 1(c) configuration] from the negative sample magnetization, right-handed laser helicity XAS [Fig. 1(b) configuration], defining the points called XMCD antiparallel (XMCD$_{ant}$).

The XAS signals [inset of Figs. 2(a) and 2(b)] for the different configurations (*par* and *ant*), can be directly compared with results obtained by Dalla Longa *et al.*[13] using visible pump and probe pulses. The pump polarization response equivalent to the nonmagnetic response in such work[13] is obtained by averaging XAS$_{\sigma+,M+}$ and XAS$_{\sigma+,M-}$ (or XAS$_{\sigma-,M+}$ and XAS$_{\sigma-,M-}$). In the present measurements XAS$_{\sigma+,M+}$ and XAS$_{\sigma+,M-}$ (or XAS$_{\sigma-,M+}$ and XAS$_{\sigma-,M-}$) signals are just reversed in sign within the statistical error, so that we can rule out any nonmagnetic pump polarization related signal. Finally, we can see in Fig. 2(b) that the Co-L_3 XMCD$_{par}$ (or XMCD$_{ant}$) signal does not show any significant increase (or decrease) during the ultrafast quench of the global Co-L_3 XMCD, and actually both signals are identical within the measurement statistics. This means that we cannot resolve pump polarization induced magnetic signal.

IV. DISCUSSION

At this point we should consider whether the effect of the angular momentum photon transfer to the orbital momentum of the electrons is too small to be seen by our measurements. To answer this question, the amount of angular momentum transferred to the magnetic layer can be calculated. The calculation estimates the amount of energy the $Co_{0.5}Pd_{0.5}$ film absorbed during our pump-probe experiment. We used the refractive indices tables given in literature[23] and a Maxwell-Garnett[24] approximation to estimate the effective refractive index of $Co_{0.5}Pd_{0.5}$. With this, we can estimate the proportion of laser absorbed in the magnetic $Co_{0.5}Pd_{0.5}$ layer by classical optics,[25] knowing that the refractive indices do not change significantly during the laser pump pulses. It was verified on our sample, by using a pump-probe setup, that the changes in dynamic transmission/reflection intensities are in the 10^{-2} range. Given the complexity of our thin film grown on Si_3N_4, we have to consider the contributions of the different layers (capping layer, magnetic film, and buffer layer) and of the interfaces between them. First, the reflectivity of the Cr capping layer is around 65% of the incident beam. Then, the absorption of this layer takes 5%. The reflection on the $Cr/Co_{0.5}Pd_{0.5}$ interface is small, so we are going to disregard the multiple bounces on the Cr layer. Finally, the magnetic layer absorbs 20% of the incident beam, transmits 9% to the Cu buffer layer, and again a negligible intensity is reflected back by the $Co_{0.5}Pd_{0.5}/Cu$ interface. At a fluence of 12 mJ/cm^2, and with a wavelength of 790 nm, the pump laser delivers 4.8×10^{16} photons/cm^2, which leads to a number of absorbed photons in the ferromagnetic layer per surface unit of 10^{16} photons/cm^2. The $Co_{0.5}Pd_{0.5}$ film contains an atomic surface density of $\sim 10^{17}$ atoms/cm^2, considering a fcc structure with an estimated lattice parameter of 0.38 nm.[26] Thus, the magnetic layer absorbs $\sim$0.1 laser photons per atom. These numbers are

in qualitative agreement with recent estimations by Si and Zhang for Ni films under similar experimental conditions.[27]

Each absorbed photon transfers an angular momentum of $\hbar$ to the system. Assuming that the transfer is done toward the orbital moment L_z of the electrons, the laser pump should change the mean orbital momentum of Co by $\pm 0.1\ \hbar$/atom. The transfer should take place during the interval Δt where the laser interacts with the magnetic film, i.e., the pump pulse duration of 60 fs. However, to compare with experimental measurements the x-ray probe duration of 100 fs has to be taken into account leading to a value $\Delta t_{\text{eff}} = 130$ fs. This value results from the convolution between x-ray pulse duration and laser pulse duration, combined with the jitter between them. In our film, we determined a static value of L_z as 0.24 $\hbar$/atom, and the spin momentum of $S_z = 0.78\ \hbar$/atom in previous measurements.[17] The XMCD signal at the Co-L_3 edge is proportional to $2L_z + S_z$. Then, after the laser pump pulse has arrived, it is expected that the sample undergoes an increase (if the laser helicity is in the same direction of L_z) or decrease (in the opposite case) on the Co-L_3 XMCD signal of $\pm 0.2\ \hbar$/atom. It should be considered here that, due to the optical selection rules, optical excitations from the pump pulse mainly involve interband transitions from occupied states with d symmetry toward empty states with p symmetry and vice versa (transitions involving s states have lower probability and are neglected). Therefore, at initial delays, we cannot exclude that a part of the angular momentum is transferred to p electrons, what is not probed by our measurement. However, we point out that due to the large difference in density of p and d states, the excited p states will have fast relaxation times to d states (few femtoseconds; see Ref. 28) and will accordingly transfer their angular momentum to the d orbitals (since angular momentum is conserved in electron-electron scattering processes). Thus the occurrence of optically excited p states at initial delays should not prevent us from observing the transferred angular momentum using time-resolved XMCD.

Therefore, for simplicity, we first assume that the angular momentum injected by the pump pulse is converted into Co orbital momentum L_z without further relaxation and probed by time-resolved XMCD. The corresponding simulated dynamics shown in Fig. 3(a) considers the model reported in Ref. 17 for $L_z(t)$ in the CoPd alloy (black line) and the situation where angular contribution from the laser field is either additive for parallel pumping (continuous blue line) or subtractive for antiparallel pumping (doted blue line). Note that this description is equivalent to assuming infinite lifetime (i.e., $\gg$1 ps in the present context) of the transferred orbital moments. In order to compare the simulated dynamics with our XMCD data at the Co-L_3 edge we have to transform the evolution of L_z [Fig. 3(a)] into $2L_z + S_z$ (Fig. 4), which is proportional to the measured Co-L_3 XMCD data.

As shown by the recent *ab initio* calculations from Carva,[20] an effective integration over the Co-L_3 XMCD peak must be done in order to apply the sum rules[18] at the ultrashort (<1 ps) time scales. The low energy resolution of the zone plate (5 eV) used in our experiment ensures that an integrated signal >5 eV is measured.[17] This way we can consider the Co-L_3 XMCD dynamics as proportional to $2L_z + S_z$. In this case, the difference between the two simulated dynamics in Fig. 4 (blue

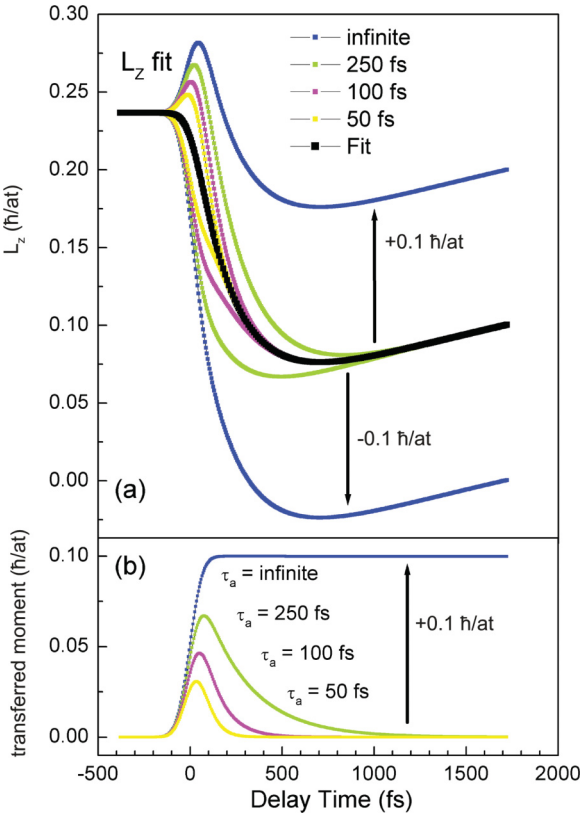

FIG. 3. (Color online) Model describing the ultrafast transfer of the angular moment of the polarized IR laser light pulse to the orbital moment of Co. (a) Dynamics of the orbital moment. The black line is the simulated demagnetization of L_z using the parameters of Ref. 17 where linear polarization of the light is used and pump polarization effects are absent. In addition to this, colored lines assume that the polarized laser lights $\sigma+$ (or $\sigma-$) transfer their angular momentum ($\pm 0.1\ \hbar$/atom) to the electronic system, with different relaxation times τ_a of the transferred moment equal to infinite (blue), 250 (green), 100 (magenta), and 50 (yellow) fs, respectively. (b) Simulation of the injected angular moment and the corresponding dynamics where a Gaussian instrumental broadening of 130 fs FWHM was included. The relaxation is simulated by exponential functions with characteristic times τ_a. The color codes are identical to Fig. 3(a).

lines) is clearly beyond the experimental errors of our data and should have been observed in Fig. 2(b). We conclude from our observations that there is a fast relaxation of the injected orbital moment, precluding any observation by means of time-resolved XMCD in the present experimental conditions. These considerations suggest that the mechanism for the relaxation of angular momentum we are dealing with is connected to the general problem of dissipation of angular momentum during the ultrafast demagnetization. This relaxation can be produced via the excitation of phonons[29] or interaction with the photon field.[5,30] In order to put some constraints on this effect, we assume an ultrafast relaxation process of the injected angular momentum according to a single exponential function with a characteristic time τ_a. The corresponding dynamics is illustrated in Fig. 3(b) where a Gaussian instrumental broadening of 130 fs FWHM was included to take into account the finite x-ray and IR pulse duration. Different values of τ_a

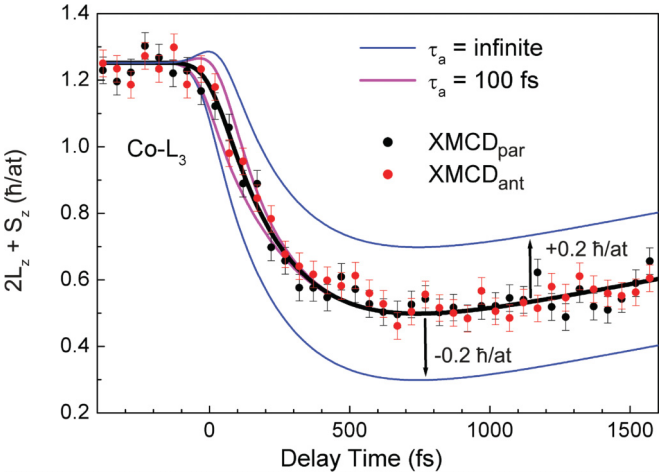

FIG. 4. (Color online) Superposed experimental and simple model for $2L_z + S_z$ ultrafast dynamics, which is proportional to the Co-L_3 dynamic, using circular IR light as a pump (see text for details). Comparing our $2L_z + S_z$ dynamic with the different lifetimes of dissipation of the angular moment we should have observed a difference between the two different circular polarizations of the light if $\tau_a > 100$ fs.

are proposed in Fig. 3(b) ranging from 50 fs to infinite. The Gaussian broadened exponential functions corresponding to the angular moment transfer ($\pm 0.1\ \hbar$/atom) combined with different characteristic orbital moment relaxation times τ_a, are finally combined with the ultrafast dynamic of the orbital moment $L_z(t)$ in Fig. 3(a). Respecting the color codes we can directly follow the effect of reducing the relaxation time to 50 fs on the ultrafast dynamic of $L_z(t)$.

In order to make a direct comparison with the magnetization dynamics, the vertical scale in Fig. 3 is set in unit $\hbar$/atom. In order to compare the simulated dynamics with our XMCD data we transform in Fig. 4 the simulations to the XMCD signal at the Co-L_3 edge using the same color codes. Finally, comparing in Fig. 4 the data and the proposed simple transfer and relaxation model, we can establish an approximate upper limit for the relaxation time of the transferred orbital moment: $\tau_a \leqslant 100$ fs.

We can now consider different mechanisms and possible baths where the orbital moment could transfer the moment with relaxation times of $\tau_a \leqslant 100$ fs. The first mechanism considers that the injected orbital moment does relax toward the "regular" magnetic momentum bath, as for instance, S. This is not the case as shown by our data, otherwise the XMCD dynamics measured at the Co-L_3 edge would have been different after pumping the film by $\sigma+$ or $\sigma-$ polarized photons (because XMCD at the Co-L_3 edge is proportional to $2L_z + S_z$), what is not observed in Fig. 4. The second possibility involves electron-phonon-mediated spin-flip scattering in the ultrafast time scale as recently suggested.[31] Though the suitability of this Elliot-Yafet mechanism to describe quantitatively the ultrafast demagnetization is still debated, we note that a recent first-principle study highlights the role of nonthermal electron population in this relaxation process,[32] which corresponds to the context of the present observation. We thus suggest that the "excess" moment in L_z achieved by circular pumping is transferred during the first 100 fs. This suggestion implies that all these relaxation and scattering mechanisms take place in the ultrafast time scales ($\leqslant$100 fs) in order to be compatible with our model and data.

V. CONCLUSIONS

We have presented experimental time-resolved XMCD measurements describing the ultrafast demagnetization process of a CoPd ferromagnetic film excited by circular polarized IR laser light. We extracted the XMCD signal in order to investigate angular momentum transfer. This effect was, however, not detected.

Our estimate shows that with the pump laser fluence we have used (allowing for a dynamical drop of the magnetization by a factor of 2), the circularly polarized pump photons transfer to the ferromagnetic film an angular momentum of about 0.1 $\hbar$/atom, which should be enough to be seen either by an intensity difference or by a time splitting of the parallel and antiparallel polarization geometry demagnetization processes.[7] Considering the finite time resolution of our experiment and a simple model predicting the dynamics of Co-L_3 as a function of the polarization of the light, the results have to be discussed considering transfer and dissipation that are restricted to time scales shorter than 100 fs. Our data are thus compatible with an ultrafast relaxation mechanism of the angular moment $L_z(t)$, shorter than 100 fs. This would explain why this angular momentum transfer is not observable in our experiment. This result is nevertheless of importance since it gives direct access to important indications about the upper limit for the time scales of dissipation processes of angular momentum, which is a central issue for magnetization dynamics. We therefore foresee that improved temporal resolution would allow unraveling the relevant mechanisms.

It also shows the interest of XMCD in the soft x-ray range for such studies since the spin and orbit part of the magnetic moment can be probed in a quantitative manner. Moreover, the use of pump and probe pulses with very different wavelengths prevents the appearance of optical effects that would hide the present angular moment dynamics at very short time scales.[12,13] The recent development of soft x-ray sources with resolutions down to a few tens of femtoseconds or less[33,34] therefore open exciting prospects for the present study.

*victor.lopez-flores@ipcms.unistra.fr
†christine.boeglin@ipcms.unistra.fr

[1] E. Beaurepaire, J. C. Merle, A. Daunois, and J. Y. Bigot, Phys. Rev. Lett. **76**, 4250 (1996).
[2] J. Y. Bigot, M. Vomir, and E. Beaurepaire, Nat. Phys. **5**, 515 (2009).
[3] A. V. Kimel, A. Kirilyuk, P. A. Usachev, R. V. Pisarev, A. M. Balbashov, and T. Rasing, Nature (London) **435**, 655 (2005).

[4]C. D. Stanciu, F. Hansteen, A. V. Kimel, A. Kirilyuk, A. Tsukamoto, A. Itoh, and T. Rasing, Phys. Rev. Lett. **99**, 047601 (2007).
[5]G. P. Zhang, Y. Bai, W. Huebner, G. Lefkidis, and T. F. George, J. Appl. Phys. **103**, 07B113 (2008).
[6]A. Scholl, L. Baumgarten, R. Jacquemin, and W. Eberhardt, Phys. Rev. Lett. **79**, 5146 (1997).
[7]B. Koopmans, M. van Kampen, J. T. Kohlhepp, and W. J. M. de Jonge, Phys. Rev. Lett. **85**, 844 (2000).
[8]L. Guidoni, E. Beaurepaire, and J. Y. Bigot, Phys. Rev. Lett. **89**, 017401 (2002).
[9]H. S. Rhie, H. A. Dürr, and W. Eberhardt, Phys. Rev. Lett. **90**, 247201 (2003).
[10]A. Kirilyuk, A. V. Kimel, and T. Rasing, Rev. Mod. Phys. **82**, 2731 (2010).
[11]F. Meier and B. P. Zakharchenya, *Optical Orientation* (North-Holland, Amsterdam, 1984).
[12]R. Wilks, R. J. Hicken, M. Ali, B. J. Hickey, J. D. R. Buchanan, A. T. G. Pym, and B. K. Tanner, J. Appl. Phys. **95**, 7441 (2004).
[13]F. Dalla Longa, J. T. Kohlhepp, W. J. M. de Jonge, and B. Koopmans, Phys. Rev. B **75**, 224431 (2007).
[14]A. Weber, F. Pressacco, S. Günther, E. Mancini, P. M. Oppeneer, and C. H. Back, Phys. Rev. B **84**, 132412 (2011).
[15]C. Stamm, T. Kachel, N. Pontius, R. Mitzner, T. Quast, K. Holldack, S. Khan, C. Lupulescu, E. F. Aziz, M. Wietstruk, H. A. Durr, and W. Eberhardt, Nature Mater. **6**, 740 (2007).
[16]C. Stamm, N. Pontius, T. Kachel, M. Wietstruk, and H. A. Dürr, Phys. Rev. B **81**, 104425 (2010).
[17]C. Boeglin, E. Beaurepaire, V. Halté, V. López-Flores, C. Stamm, N. Pontius, H. A. Dürr, and J. Y. Bigot, Nature (London) **465**, 458 (2010).
[18]B. T. Thole, P. Carra, F. Sette, and G. van der Laan, Phys. Rev. Lett. **68**, 1943 (1992).
[19]K. Holldack, T. Kachel, S. Khan, R. Mitzner, and T. Quast, Phys. Rev. ST Accel. Beams **8**, 040704 (2005).
[20]K. Carva, D. Legut, and P. M. Oppeneer, Europhys. Lett. **86**, 57002 (2009).
[21]A. G. Michette, S. J. Pfauntsch, A. Erko, A. Firsov, and A. Svintsov, Opt. Commun. **245**, 249 (2005).
[22]S. Khan, K. Holldack, T. Kachel, R. Mitzner, and T. Quast, Phys. Rev. Lett. **97**, 074801 (2006).
[23]Refractive Index Database, [http://refractiveindex.info] (last accessed on Jan. 1, 2012).
[24]J. C. M. Garnett, Philos. Trans. R. Soc. London, Ser. A **203**, 385 (1904).
[25]M. Born, E. Wolf, and A. B. Bhatia, *Principles of Optics: Electromagnetic Theory of Propagation, Interference and Diffraction of Light*, 7th ed. (Cambridge University Press, Cambridge, England, 1999).
[26]L. I. Kveglis, S. M. Jarkov, G. V. Bondarenko, V. Y. Yakovchuk, and E. P. Popel, Phys. Solid State **44**, 1117 (2002).
[27]M. S. Si and G. P. Zhang, J. Phys.: Condens. Matter **22**, 076005 (2010).
[28]R. Knorren, K. H. Bennemann, R. Burgermeister, and M. Aeschlimann, Phys. Rev. B **61**, 9427 (2000).
[29]B. Koopmans, J. J. M. Ruigrok, F. D. Longa, and W. J. M. de Jonge, Phys. Rev. Lett. **95**, 267207 (2005).
[30]E. Beaurepaire, G. M. Turner, S. M. Harrel, M. C. Beard, J. Y. Bigot, and C. A. Schmuttenmaer, Appl. Phys. Lett. **84**, 3465 (2004).
[31]B. Koopmans, G. Malinowski, F. Dalla Longa, D. Steiauf, M. Faehnle, T. Roth, M. Cinchetti, and M. Aeschlimann, Nature Mater. **9**, 259 (2010).
[32]K. Carva, M. Battiato, and P. M. Oppeneer, Phys. Rev. Lett. **107**, 207201 (2011).
[33]B. Vodungbo, A. B. Sardinha, J. Gautier, G. Lambert, M. Lozano, S. Sebban, E. Meltchakov, F. Delmotte, V. López-Flores, J. Arabski, C. Boeglin, E. Beaurepaire, R. Delaunay, J. Lüning, and P. Zeitoun, Europhys. Lett. **94**, 54003 (2011).
[34]C. Gutt, S. Streit-Nierobisch, L. M. Stadler, B. Pfau, C. M. Günther, R. Könnecke, R. Frömter, A. Kobs, D. Stickler, H. P. Oepen, R. R. Fäustlin, R. Treusch, J. Feldhaus, E. Weckert, I. A. Vartanyants, M. Grunze, A. Rosenhahn, T. Wilhein, S. Eisebitt, and G. Grübel, Phys. Rev. B **81**, 100401 (2010).